Journal of Catalysis 390 (2020) 161–169

Contents lists available at ScienceDirect

Journal of Catalysis

journal homepage: www.elsevier.com/locate/jcat

Bifunctional molybdenum oxide/acid catalysts for hydroisomerization of n-heptane ☆

Justine Harmel [a], Tegan Roberts [b], Zhaorong Zhang [c], Glenn Sunley [b], Petra de Jongh [a], Krijn P. de Jong [a,*]

[a] Inorganic Chemistry and Catalysis, Debye Institute for Nanomaterials Science, Utrecht University, Universiteitsweg 99, 3584 CG Utrecht, the Netherlands
[b] Applied Chemistry and Physics Centre of Expertise, BP Group Research, c/o BP Chemicals, Saltend, Hull HU 12 8DS, UK
[c] Applied Chemistry and Physics Centre of Expertise, BP Group Research, 150 West Warenville Road, Naperville, IL 60563, USA

ARTICLE INFO

Article history:
Received 30 May 2020
Revised 31 July 2020
Accepted 1 August 2020
Available online 12 August 2020

Keywords:
Bifunctional catalysts
Mo oxide
Solid acid
Hydroisomerization

ABSTRACT

Numerus research studies focus on replacing scarce noble metals by non-noble transition metals in solid catalysts. The (de)hydrogenation function in bifunctional catalysts for hydroisomerization and hydrocracking of alkanes is usually performed by a precious metal such as Pt, or a metal sulfide such as MoS_2. In this study, we investigated the possibility of replacing Pt with a non-sulfided MoO_x catalyst in combination with a mesoporous solid acid for the hydroisomerization of *n*-heptane. MoO_x particles size as well as the preparation techniques were varied in order to identify the Mo active phase for (de) hydrogenation. We demonstrated that an optimized non-precious metal MoO_x catalyst can perform similarly to its Pt counterpart in the *n*-heptane conversion when used in combination with a mesoporous solid acid.

1. Introduction

Catalytic dewaxing is a key reaction in the refining and upgrading of hydrocarbons. It involves selective hydroisomerization of linear alkanes to branched molecules, with limited cracking to less desirable lighter products. Through hydroisomerization processes, the cold flow properties of fuels and lubricants from potentially renewable feedstocks such as Fischer-Tropsch (FT) wax are improved to meet specification [1]. Pt on solid acid is a common commercial catalyst for the hydroisomerization of hydrocarbon feedstocks, but makes use of an expensive and non-abundant noble metal. In addition, these commercial catalysts are sensitive to the presence of impurities (especially sulfur and H_2O) and to deactivation by coke deposition [2–4].

It is therefore of great interest to find active catalysts replacing Pt with non-noble metal, but up to date, this remains a challenging task [5,6]. Catalysts based on transition metals in the sulfide form, such as Co or Ni promoted MoS_2, have been studied to circumvent these drawbacks, but they are primarily employed for hydrodesulfurization, hydrodenitrification and hydrocracking of sulfur-containing heavy oil fractions [7]. This catalyst is sufficiently active only at relatively high temperatures (350–400 °C), much less selective towards isomers than Pt catalysts, and requires sulfur in the feed [8]. Preferably this is avoided in the case of FT wax upgrading, where the feedstock is sulfur free, and more generally, in line with the trend of obtaining more valuable clean products complying with the latest environmental regulations on the sulfur content of fuel [9,10].

Among the non-noble sulfide-free metal catalysts described in the literature, transition metal carbides have been extensively studied [11–13]. Early studies by Boudart and co-workers [11] showed that the performance of tungsten carbides and their properties in catalysis mimicked those of Pt, albeit at higher temperatures. In the field of hydroconversion of alkanes, unsupported bulk MoO_3 powder has been reported to be surprisingly active for hydroisomerization of heptane and hexane in studies by Ledoux and coworkers [14–20]. They attributed this performance to the formation of an oxycarbide phase of molybdenum under reaction conditions [21–24]. Other groups considered the formation of MoO_xH_y phase as a key step to generate the hydroisomerization activity.[25,26]. This active phase was also suggested by Meunier et al. after TPO studies evidenced that the activity of Mo powder catalyst does not corelate with the content of carbon in the oxycarbidic phase but rather to the presence of an oxide of Mo [27–30]. Overall, the nature of the active phase and the mechanism of the reactivity of the molybdenum have remained unclear.

Here, we report a detailed study of the preparation and performance of molybdenum oxide supported on solid acid catalysts that

☆ This publication is dedicated to the memory of Michel Che, whose work in the fields of catalysis and surface reactivity studies have been an inspiration.

* Corresponding author.
E-mail address: K.P.deJong@uu.nl (K.P. de Jong).

https://doi.org/10.1016/j.jcat.2020.08.004
0021-9517/© 2020 Published by Elsevier Inc.

exhibited Pt-like performance with both comparable activity and selectivity for hydroisomerization of *n*-heptane, as a model feedstock to study alkanes hydroconversion. The molybdenum active sites were proposed to be MoO_x, $Mo^{\delta+}$ species. The bifunctional nature of the catalyst, with Mo acting as (de)hydrogenation function and the solid acid providing the isomerization sites, was demonstrated.

2. Experimental

2.1. Catalyst preparation.

– Pt- Reference catalysts

Pt on solid acid catalysts were prepared following published procedures [31,32], which are briefly described as follows: 1 g of amorphous silica-alumina (ASA; Siralox40hpv, Sasol) of particle sizes in the range 500–212 μm was stirred in 200 ml of Milli-Q water for 30 min. Then a solution (20 ml) containing 20.05 mg of $[Pt(NH_3)_4\ (NO_3)_2]$ (Sigma) was added dropwise allowing ion exchange (IE) to take place. After 3 h of stirring, the solid was filtered, washed with Milli-Q water until a neutral pH was reached, and dried in air at 120 °C overnight. The samples were calcined under air (GHSV ~ 3000 h^{-1}) at 350 °C for 2 h with a ramp of 0.2 °C min^{-1} and reduced in H_2 (GHSV ~ 3000 h^{-1}) at 600 °C for 3 h, with a ramp of 3 °C min^{-1}. ICP analysis displayed a loading of 0.49 wt% Pt. All the platinum reference catalysts discussed in the paper were prepared on the corresponding support by ion exchange as described in Pt-ASA procedure using the same Pt precursor with the exception of 5 wt% Pt-Al_2O_3 (Sigma-Aldrich) that was bought and used as such.

A series of supported non-noble metal catalysts was prepared. An overview of all samples can be found in Table 1 in the results section.

– *MoO_x/ASA (IWI)*

A Mo catalyst supported on Siralox40hpv was prepared by incipient wetness impregnation using an aqueous solution of ammonium molybdate, $Mo_7O_{24}(NH_4)_6{\cdot}4H_2O$ First, 1.0 g of support material (ASA, pore volume of 1.6 $cm^3\ g^{-1}$) was dried under vacuum at 80 °C for 1 h, thereafter the incipient wetness impregnation was performed at room temperature with a Mo aqueous solution with the appropriate concentration (Mo target loading of 13 wt% or 5%). The powder was dried overnight at 120 °C and further dried at 150 °C under N_2 flow (GHSV ~ 3000 h^{-1}) with a ramp of 2 °C min^{-1} and reduced at 385 °C for 6 h under H_2 flow with a ramp of 0.2 °C min^{-1} (GHSV ~ 3000 h^{-1}). The resulting catalyst was designated Mo-ASA (IWI). After reduction, the catalyst was passivated by exposure to air prior to characterization.

– *$CoMoO_x$/ASA (IWI) and $NiMoO_x$/ASA (IWI)*

Mo-ASA (IWI) was subsequently impregnated with either a Co or Ni nitrate salt ($Co(NO_3)_2{\cdot}6H_2O$ or $Ni(NO_3)_2{\cdot}6H_2O$, Acros 99%). The powder was dried overnight at 120 °C and further dried at 150 °C under N_2 flow (GHSV ~ 3000 h^{-1}) with a ramp of 2 °C min^{-1}. and reduced at 385 °C for 6 h under H_2 flow with a ramp of 0.2 °C min^{-1} (GHSV ~ 3000 h^{-1}). The resulting catalyst was designated $CoMoO_x$/ASA.

– *MoO_x/ASA (PM)*

A MoO_x/ASA (PM) catalyst was prepared by a physical mixture (PM) of a commercial MoO_3 powder (Acros, 99%+ purity with XRD pattern conforming to MoO_3 structure) together with Siralox40hpv ASA. The amount of MoO_3 powder was adjusted to obtain a catalyst with a final Mo loading of 13 wt% with Siralox40hpv. The mixture was then pelletized at 650 kg cm^2 with a press, grinded in a mortar and sieved to a 212–500 μm fraction. The catalyst was then dried at 150 °C under N_2 flow (GHSV ~ 3000 h^{-1}) with a ramp of 2 °C min^{-1} and reduced at 385 °C for 6 h under H_2 flow with a ramp of 0.2 °C min^{-1} (GHSV ~ 3000 h^{-1}).

– *MoO_x/ASA (acac)*

A MoO_x/ASA (acac) catalyst was prepared by titration of the OH^- group with $MoO_2(acac)_2$ on of the ASA Siralox40hpv following pub-

Table 1
Mo and Pt catalysts characteristics after reduction.

	Catalyst	Solid acid	Preparation technique	Metal loading (%wt) [a]	Metal particle size (nm)	N acid (mmol/g) [c]	N metal (mmol/g) [d]	N metal surface[e]/Nacid
1	*Pt/ASA*	ASA	IE	0.6	1.1	0.45	0.03	0.067
2	*MoO_x/ASA (IWI)*	ASA	IWI	5	1.5	0.47	0.52	1.08
3	*MoO_x/ASA (IWI)*	ASA	IWI	13	1.4	0.58	1.35	2.81
4	*$CoMoO_x$/ASA (IWI)*	ASA	IWI	5	nd	0.58	1.35	–
5	*$NiMoO_x$/ASA (IWI)*	ASA	IWI	5	nd	0.58	1.35	–
6	*MoO_x/ASA (acac)*	ASA	(–OH Exchange)	5	0.9	0.43	0.58	1.21
7	*MoO_x/ASA (PM)*	ASA	PM	5	40[b]	0.47	0.52	0.05
8	*MoO_x/ASA (PM)*	ASA	PM	13	38[b]	0.47	1.35	0.13
9	*Mo_2C/ASA(PM)*	ASA	PM	13	nd	nd	–	–
10	*MoO_3 powder*	None	Commercial	67	–	–	6.98	–
11	*MoO_x/Al_2O_3*	Puralox	PM	13	0.9	nd	1.35	–
12	*Pt/Al_2O_3*	Al_2O_3	Commercial	5	nd	–	0.25	–
13	*MoO_x/SBA-15*	SBA-15	PM	13	29[b]	0.02	1.35	–
14	*Pt/SBA-15*	SBA-15	IE	0.5	1.3	0.02	0.03	–
15	*MoO_x/Al-SBA-15*	Al-SBA-15	PM	13	40[b]	0.20	1.35	0.30
16	*MoO_x/Al-SBA-15*	Al-SBA-15	IWI	13	1.5	0.20	1.35	5.28
17	*MoO_x/Al-SBA-15*	Al-SBA-15	IWI ($MoO_2(acac)_2$)	6	3	0.20	0.58	1.27
18	*Pt/Al-SBA-15*	Al-SBA-15	IE	0.5	1.15	0.20	0.03	0.16
19	*Pt/SBA-15*	SBA-15	IE	0.5	1.6	0.02	0.03	–

[a] Metal loading determined by ICP for platinum or molybdenum catalysts.
[b] Crystallite size determined by XRD line broadening based on MoO_2 crystallites with these catalysts or TEM for all other samples.
[c] Total number of acid sites determined by integration of NH3-TPD profiles.
[d] Total molar number of metal sites based on either Pt or MoO_2 species.
[e] $n_{Metal\ surface}$ is the total molar amount of Pt or MoO_2 on the surface of the particles determined based on the dispersion assuming either in Pt or MoO_2 form. nd stands for not determined.

lished procedure [33]. The OH groups exchange with the Mo precursor $MoO_2(acac)_2$, which should result in the grafting of $MoO_2(OH)_2$ species on the alumina rich domains of the silica-alumina. Briefly, a solution of $MoO_2(acac)_2$ in EtOH (20 ml) was left equilibrate with the ASA powder (1 g dried at 120 °C beforehand to remove water) for 2 weeks stirring at RT, the solution changed color from light orange to green. The powder was washed 3 times with 20 ml of EtOH, and then dried at 150 °C under N_2 flow (GHSV ~ 3000 h^{-1}) with a ramp of 2 °C min^{-1} and reduced at 385 °C for 6 h under H_2 flow with a ramp of 0.2 °C min^{-1} (GHSV ~ 3000 h^{-1}). ICP analysis showed a loading of 5.6 wt% Mo. The resulting catalyst was designated *MoO_x/ASA (acac).*

– *SBA-15 and Al-SBA-15*

Procedures for the synthesis of SBA and Al-SBA-15 solid acid have been reported in detail elsewhere [31]. Briefly, mesoporous rod-shaped SBA-15 was prepared with a molar composition of the gel such as P123:TEOS:HCl:H_2O = 0.017:1.0:5.9:192.35 SBA-15 rods of 0.2 × 0.5–2 μm were obtained. The grafting of Al on SBA-15 (aimed Si/Al = 20) was then performed. Al isopropoxide, AlIJO-iPr)3 (Aldrich) (0.83 mmol or 1.66 mmol) was dissolved in anhydrous cyclohexane (Fluka) under N_2 atmosphere. The SBA-15 support (1 g), dried at 250 °C for 2 h prior to the reaction, was quickly transferred to the Al solution. The suspension was stirred overnight before filtration and washing with cyclohexane. The solid was then dried overnight at 120 °C and calcined under static air at 500 °C for 4 h (1 °C min^{-1} ramp). The Al content of the final material was determined by ICP/AES and EDX.

– *Physical mixtures*

The physical mixtures were prepared following the procedure described for MoO_x/ASA (PM), using as mesoporous material SBA-15 SiO_2, Al-SBA-15, and Al_2O_3 (Sasol Pural TH100-150). Main characteristics of the porous support are given in Table SI.1.

Mo_2C/ASA (PM) was prepared as PM of Mo_2C (Sigma-Aldrich 99 +%) with ASA (Siralox40hpv (Sasol)).

– *Physical mixtures of sieved fractions*

MoO_x catalysts with different intimacy degree between the molybdenum oxide and the ASA powder were obtained to study the influence of the preparation on the proximity between the functions:

- *MoO_x (75–212 μm) + ASA (75–212 μm):* the catalyst was obtained by hand-mixing a sieved fraction (75–212 μm) of MoO_x powder with a similar sieved fraction (75–212 μm) of ASA powder
- *MoO_x/ASA (PM)*: catalyst resulting from a mortar powder mixing of the two powders, the mixture was then pelletized at 1.5 metric tons with a press, ground in a mortar and sieved to a 75–212 μm fraction (Physical mixture)
- *MoO_x/ASA (Extrudate)*: A catalyst was prepared by extrusion in D1/8″ cylinder of MoO_3 powder mixed together with ASA powder, using DI water as the formulation medium. The extrudate was dried overnight at 120 °C and further dried at 150 °C under N_2 flow (GHSV ~ 3000 h^{-1}) with a ramp of 2 °C.min^{-1} and reduced at 385 °C for 6 h under H_2 flow with a ramp of 0.2 °C.min^{-1} (GHSV ~ 3000 h^{-1}). The extrudate was then crushed into powder in a mortar and sieved to a 75–212 μm fraction.

2.2. Catalyst characterization.

N_2 physisorption was performed at −196 °C on a Micromeritics TriStar 3000 system. Prior to analysis, the samples were outgassed in vacuum at 400 °C for 20 h. The total pore volume was determined at p/p_0 = 0.995.

The Pt content was determined by inductively coupled plasma-optical emission spectroscopy (ICP-OES) at Mikroanalytisches Laboratorium Kolbe. The analyses were carried out in an ICP-OES Perkin-Elmer Analyst 200 spectrometer, after a digestion procedure (Company confidential process).

H_2-Chemisorption was measured on a Micromeritics ASAP 2020 instrument. Prior to the measurement the sample was reduced at 350 °C in H_2 for 2 h (heating ramp of 1 °C min^{-1}) and evacuated. The chemisorption of H_2 was then conducted at 35 °C.

Temperature-programmed desorption (TPD) of ammonia was carried out on a Micromeritics AutoChem II equipped with a thermal conductivity detector (TCD). Typically, 100 mg of catalyst was dried in a flow of He for 15 min at 600 °C, with a heating ramp of 10 °C min^{-1}. The temperature was then decreased to 100 °C and 10 vol% ammonia in He was adsorbed in a pulse-wise manner (10 ml.min^{-1}) until oversaturation. Thereafter the physisorbed ammonia was removed by flowing He for 2 h at 100 °C. The ammonia desorption was monitored from 100 °C to 600 °C with a ramp of 10 °C min^{-1}.

Pyridine adsorption/desorption and infrared measurements were conducted on a ThermoFisher Nicolet i5 spectrometer (32 scans, 4 cm^{-1} resolution, DTGS detector). The pellet was dried by heating in the cell at 200 °C (ramp of 10 °C min^{-1}) for 2 h, and then cooled down to 50 °C. At that temperature, pyridine (99.9%, Sigma–Aldrich) vapor was introduced into the cell to an equilibrium pressure set to 10 mbar. Pyridine was then desorbed by increasing temperature at a pressure of 1.10^{-5} bar.

Transmission electron microscopy (TEM) measurements, high angle annular dark field scanning transmission electron microscopy (HAADF-STEM) measurements, combined with energy dispersive X-ray spectroscopy (EDX) measurements, were performed on an FEI Talos™ F200X transmission electron microscope, using an X-FEG electron source and a Super-X™ EDX detector. Prior to the measurements the catalysts were embedded in Epofix resin and thin-sectioned into ~70 nm slices using a Reichert-Jung Ultracut E ultramicrotome with a Diatome Ultra 35° diamond knife. These slices were deposited on a carbon-coated copper TEM grid.

Temperature programmed reduction (TPR) analyses were performed using a Micromeritics Autochem2990 instrument, after a drying step at 120 °C for 1 h in Ar flow followed by reduction from room temperature up to 800 °C (5 °C min^{-1}) in a 5 vol% H_2/Ar flow. Raman spectroscopy measurements were performed on a Renishaw Raman microscope, using 638 nm diode laser excitation through a ×50 objective (0.5 numerical aperture).

2.3. Catalysis

2.3.1. Hydroisomerization of n-heptane

The hydroisomerization of *n*-heptane was carried out in a 16-parallel fixed-bed-reactor catalytic setup (Flowrence, Avantium). An HPLC pump was used to inject the *n*-heptane (ACROS Organics, purity > 99.5%) into the feed distribution system. The reaction products were analyzed by online gas chromatography instrument (Agilent 7890A), with a capillary column (Agilent J&W PoraBOND Q) and flame ionization detector (FID). 25–50 mg of catalyst (fraction 75–212 μm) was loaded for each reactor (2 mm internal diameter). Prior to the reaction, the catalysts were dried in a flow of He at 120 °C for 1 h and reduced in H_2/He flow at 300 °C for 2 h, with a heating ramp of 3 °C min^{-1}. The 16 parallel reactors were then pressurized to 10 bar under H_2 flow and a total flow of *n*-heptane of 29 μl min^{-1} was introduced. Under these conditions the molar ratio of H_2 to *n*-heptane was 10 and WHSV = 1.15 $g_{C7}.g^{-1}_{catalyst.}$ h^{-1}. With $g_{catalyst,}$ we refer to the total

mass of catalyst sieve fraction loaded in the reactor. The hydroisomerization reaction was carried out in the range 200–400 °C. To check the stability of the catalysts, the experiment was followed by a 'back check' by decreasing the temperature to 350 °C for 24 h at the end of the temperature range and compared with the first results obtained at that temperature. The total C7 isomer yield was determined by the sum of the mono-branched and di-branched C7 isomer products and the total C7 cracking yield was determined by the sum of the *i*-C4 and *n*-C3 cracking products.

3. Results and discussion

3.1. Characterization of the catalysts

Molybdenum oxide catalysts supported on supports with different porosity and acidity were obtained, by varying the preparation method and the Mo precursor. The Mo oxides catalysts are referred to as MoO_x as the oxidation state is not fixed. The characteristics of the Mo catalysts and the Pt reference catalysts are summarized in Table 1. In the case of Pt catalysts, key parameters for obtaining an ideal bi-functional catalysts have been found to be the ratio between the number of Pt sites and acid sites, the distance between both sites, and the Pt particle size [34,35]. The same parameters were investigated here for MoO_x-based bi-functional catalysts.

NH_3-TPD was used to evaluate changes in the number and strength of the acid sites upon Mo deposition on amorphous silica-alumina. All preparation techniques resulted in a slight shift of the acidity towards lower temperature desorption (and hence weaker acidity), but the total amount of acid sites remained similar or slightly higher (See Fig. 1 and Table 1). In the case of MoO_x/ASA (acac) the total number of acid sites is slightly decreased (green line), which can be explained by the grafting procedure taking place on the surface of the solid acid.

HAADF-STEM images of selected samples are presented in Fig. 2 and allowed to determine the particle size distribution. In the case of the samples prepared by IWI, both MoO_x/ASA (IWI) and MoO_x/Al_2O_3 (IWI) contained nanoparticles (NPs) of MoO_x species (~1 nm in size) dispersed on the support. MoO_x/ASA(PM) exhibited large crystals of MoO_x with selected area exhibiting large MoO_x particles and some smaller particles. In the case of MoO_x/ASA (acac), the calcination and reduction treatment did not result on NPs formation, as no NPs could be observed by STEM, but the presence of dispersed Mo species over the support could be detected by EDX mapping of the alumina rich area of the ASA (See SI Fig. 1).

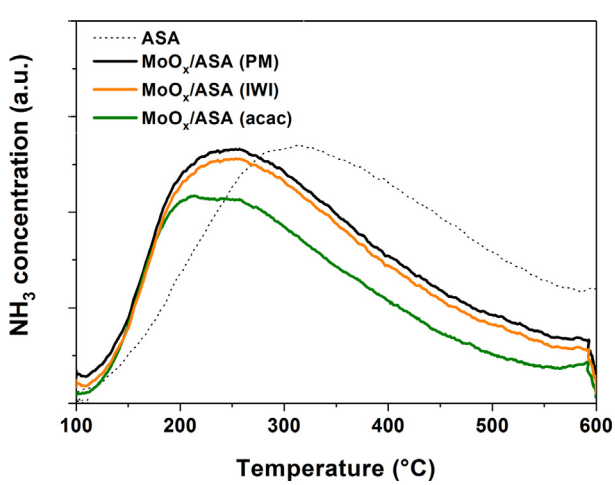

Fig. 1. NH3– TPD profile of ASA (dotted line); MoO_x/ASA (PM) (black line); MoO_x/ASA (IWI) (orange line) and MoO_x/ASA (acac) (green line).

With this set of catalysts, the MoO_x particle size supported on an amorphous silica-alumina support was ranging from atomic species in the case of the MoO_x/ASA (acac), to 30–40 nm crystals in the case of MoO_x/ASA(PM) catalyst.

XRD of MoO_x /ASA (IWI) did not show any diffraction peak that could be attributed to Mo or MoO_x crystallites because of the small size of the NPs (1.4 nm by HAADF-STEM). In the case of MoO_x/ASA (PM), the XRD pattern clearly showed diffraction peaks that could be attributed to MoO_2 with a domain size of about 40 nm (Fig. 3).

The oxidation state of the catalyst was also studied by H_2-TPR (Fig SI.2 TPR), confirming the presence of MoO_2 species.

3.2. n-heptane hydroisomerization

3.2.1. Catalytic study of the oxide catalyst prepared via impregnation

MoO_x catalysts and combinations of Mo catalysts with Co or Ni were prepared by (consecutive) incipient wetness impregnation of a mesoporous (silica-alumina) support. Table 1 (Row 3–5) reports the main characteristics of the prepared catalysts. The influence of the presence of cobalt (CoMo/ASA with 4 wt% Co) or nickel (NiMo/ASA with 4 wt% Ni) on Mo was studied for *n*-heptane conversion. Both NiMo and CoMo catalysts showed a high activity for the conversion of *n*-heptane, although the product distribution is characteristic of hydrogenolysis with a methane yield rapidly reaching 100% with increasing reaction temperature. (Fig. 4.) A high selectivity to methane for non-sulfided CoMo catalyst via hydrogenolysis of alkanes has been reported earlier [36,37]. We attribute this behavior to metallic cobalt or nickel sites catalyzing hydrogenolysis, resulting in methane and normal alkanes. Interestingly, MoO_x showed both appreciable *n*-heptane conversion and selectivity toward C7 alkane isomers, although the activity was shifted to higher temperature compared to the Pt/ASA reference catalyst. For Mo/ASA prepared by impregnation a similar level of *n*-heptane conversion is reached at ~40 °C above the temperature required in the case of Pt/ASA. The isomer yield is nevertheless significant, up to 44%, against 65% for Pt/ASA. Neither Pt/ASA nor MoO_x/ASA (IWI) catalysts resulted in significant yields of methane or hexane, suggesting that Mo oxide itself does not significantly contribute to hydrogenolysis. The rest of the paper will focus on catalysts containing Mo oxide species only.

3.2.2. Preparation method for Mo oxide

In order to gain understanding on the Mo oxide behavior for *n*-heptane hydroisomerization, catalysts were prepared by different preparation techniques resulting in samples with MoO_x particle sizes ranging from 1 nm to 40 nm, but also to different loadings and dispersion of the Mo species on the support. (Table 1 Row 3; 6–8) The catalytic properties of these Mo oxide catalysts in the *n*-heptane hydroconversion, with activity, isomerization and cracking yield are reported in Fig. 5. Interestingly, all Mo oxide supported catalysts showed both activity and formation of C7 alkane isomers.

MoO_x/ASA (PM) (13 wt% Mo) catalyst shows a very similar activity conversion profile and selectivity yield toward C7 isomers as the Pt/ASA catalyst, with 50% conversion around 350 °C for both catalysts at the prevailing reaction conditions. The maximum C7 isomer yield was 65% for both the MoO_x/ASA (PM) sample and the Pt/ASA sample. The product distribution for these samples is detailed in Table 2 (molar distribution with carbon number other than 7 in Figure SI.3). The main products detected were 2-methylhexane and 3-methylhexane, mono-branched isomers of C7, and di-branched products (~8%), mainly di-methyl-pentane. The main by-products, obtained for both Mo and Pt catalysts, were cracking products with the amount of C3 and *iso*-C4 products indicating a conventional cracking pattern for acid catalysis over MoO_x/ASA similar to the one on Pt /ASA catalyst. This suggests that

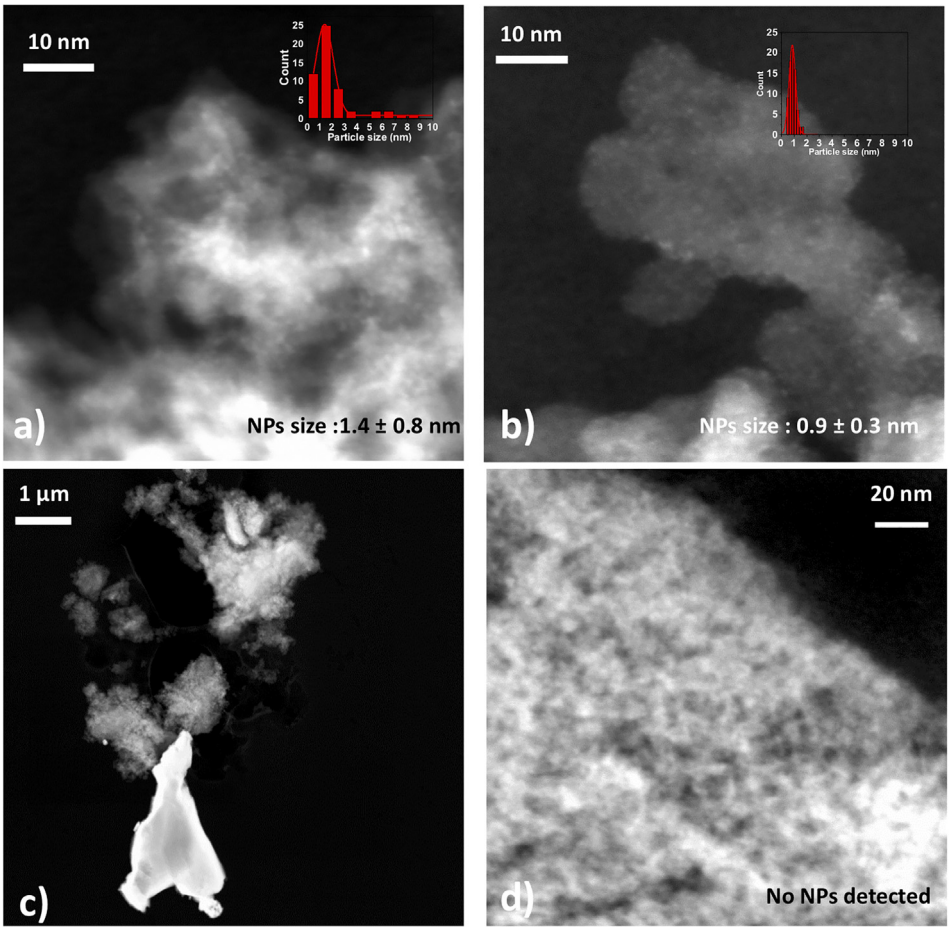

Fig. 2. HAADF-STEM image of Mo catalysts a) MoO_x/ASA (IWI), b) MoO_x/Al_2O_3 (IWI), c) MoO_x/ASA (PM) and d) MoO_x/ASA (acac),

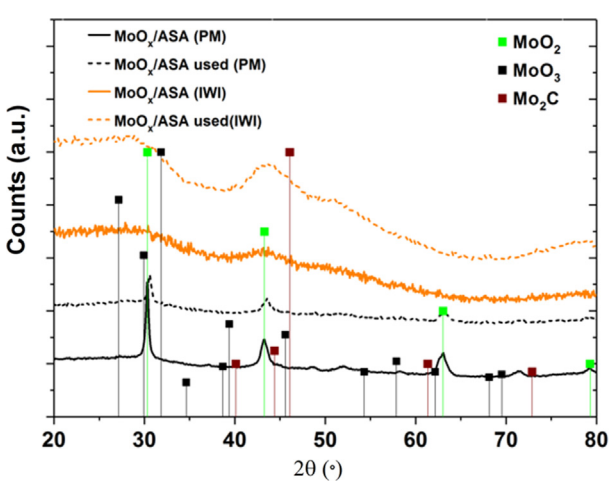

Fig. 3. XRD diffractogram of) MoO_x/ASA (PM) (reduced: black line and used (after 200 h TOS): black dotted line) and MoO_x/ASA (IWI) (reduced: orange line and used (after 200 h TOS): orange dotted line).

the global reaction mechanism on Mo catalyst is similar to that of an ideal Pt bi-functional catalyst [1].

The physical mixture of MoO_3 powder and ASA led to similar performance as the Pt/ASA catalyst. The apparent activation energy of this Mo catalyst, calculated at a *n*-heptane conversion below 20%, is around 179.1 kJ mol^{-1} which is slightly higher than the value for the optimized Pt/ASA catalyst of 167.3 kJ mol^{-1} (See Fig.SI.4).

3.2.3. Mo-oxide crystallite size effects

MoO_x particles with crystal sizes ranging from around 1 nm to 30–40 nm were studied in order to determine the size range required for optimal (de)hydrogenation activity. Surprisingly, the catalyst prepared by physical mixing and containing micrometers-sized particles (Fig. 2) exhibited both higher activity and selectivity to isomers over the range of Mo oxide particles size. MoO_x/ASA (acac), with highly dispersed Mo species also presented a high activity and selectivity, but with a maximum isomer yields of 50%. This particular catalyst was characterized by highly dispersed Mo species, as confirmed also by TEM for the catalyst used for >200 h, with no NPs detected, pointing to an active species being grafted Mo oxide species.

The activity of all Mo supported on various mesoporous ASA and alumina is summarized in Fig. 6. We can observe a clear trend of an increase of the activity with an increase of the average crystallite size.

Although all MoO_x catalysts showed significant activity and isomers formation, the one prepared by PM showed the highest yield of isomers. Therefore, we also investigated other catalysts obtained by this method. The maximum isomer yields obtained, and the temperatures needed to reach this isomer yield of these catalysts are summarized in Fig. 7 and compared with the corresponding Pt catalysts. (Isomer yields are detailed in Fig.SI.5). The acidity of the supports roughly increases from left to right; going from non-acidic silica, SBA-15 and alumina Al_2O_3 on the left to mildly acidic ASA (Al-SBA-15 and Siralox). In order to get further insight into the reactivity, detailed products distributions of selected catalysts are given in Table 2.

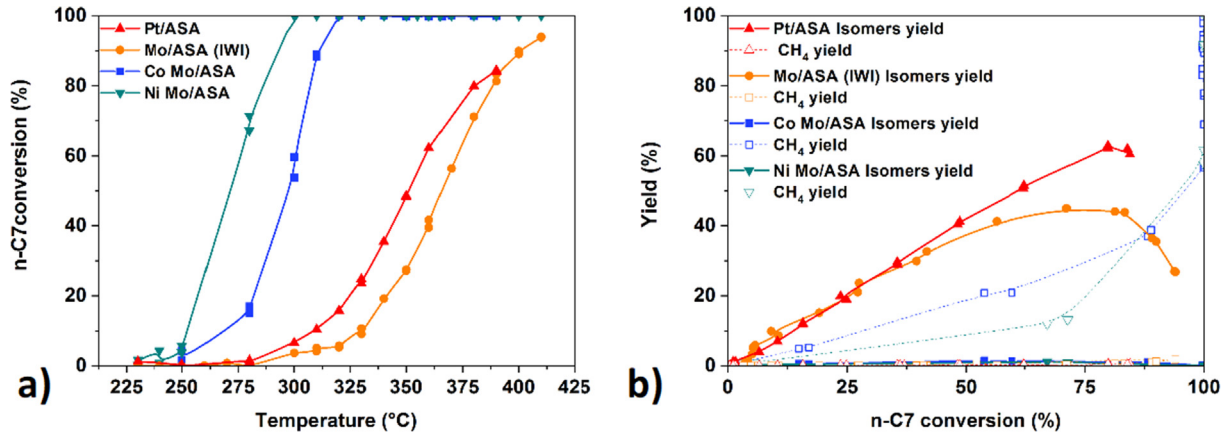

Fig. 4. a) n-heptane conversion as a function of temperature for NiMoOx/ASA; CoMoOx/ASA; MoOx/ASA and Pt/ASA catalysts b) total isomerization yield (%) and CH_4 yield (%) (Experiments were performed at a pressure of 10 bar ; H_2/n-C7 = 10/1 mol/mol; WHSV = 1.15 $g_{n\text{-}C7}.g_{catalsyt}.h^{-1}$).

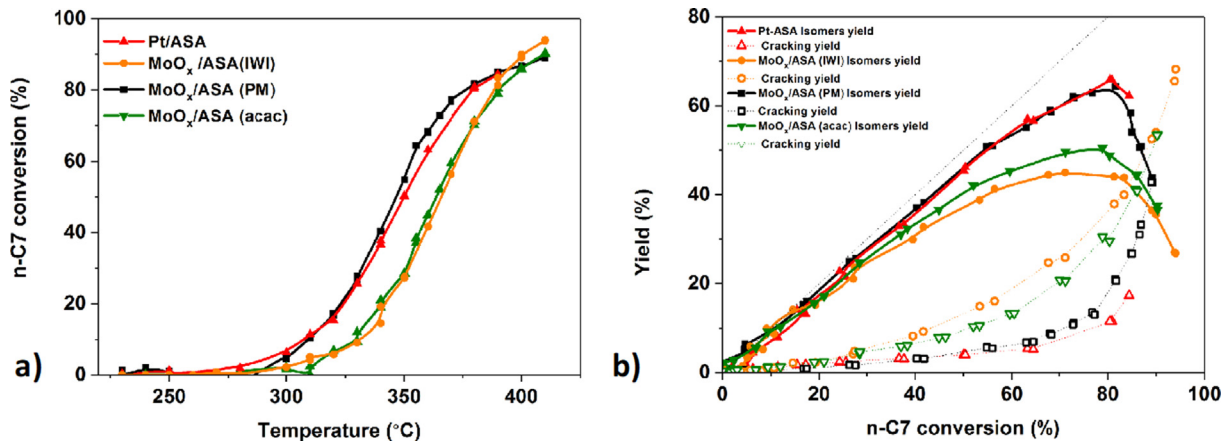

Fig. 5. a) n-heptane conversion as a function of temperature for Pt/ASA, MoO_x/ASA (prepared by impregnation (IWI) or physical mixture (PM)) and MoO_x/ASA(acac) b) Total isomers yield and total cracking yield as a function of n-heptane conversion (experiments at 10 bar, H_2/n-C7 = 10/1 mol/mol, WHSV = 1.15 $g_{n\text{-}C7}.g_{catalsyt}.h^{-1}$).

Table 2
Catalytic properties of selected representative catalysts tested; 10 bar; H_2/n-C7: 10/1 mol/mol.

Catalyst	Pt/ASA	MoO_3 powder	Mo/ASA (PM)	Mo/Al-SBA-15	Mo/Al_2O_3
Temperature (°C)	370	350	370	370	400
Conversion (%)	80.9	81.1	82	83	55.5
Isomers selectivity (%)	81	14	80	69	13.3
Mono-branched products (wt%)	57.7	28.3	57	48	8.3
Di-branched products (wt%)	8.0	3.4	7.5	4.3	0.1
Total isomer yield (wt%)	**65.7**	**31.7**	**64.5**	**52.3**	**8.4**
C1 (Hydrogenolysis) (wt%)	0.2	0.2	0.2	0.1	7.9
Total cracked products yield (wt%)	9.35	49.4	17.5	30.7	11.6
Iso-C4/C3	0.63	0.63	0.68	1.02	0.03
Cyclic products yield (wt%)	0.1	0.3	0.2	0.2	0

Focusing on the non-acidic support, Mo catalysts show slightly higher performances than the Pt ones as molybdenum species apparently provide some additional acidity to the catalyst resulting in a limited isomers formation: 10 to 15% isomers yield at high temperature 390–400 °C. In contrast, without the acidity of a support, Pt catalysts do not have the necessary bi-functionality to perform isomerization. In the case of molybdenum supported on alumina or silica-alumina, it has been reported by the group of Che that it is crucial to avoid alumina dissolution and extraction during the preparation of the supported MoO_X catalysts [38]. Our preparation technique by physically mixing should ensure that such extraction is avoided.

For mildly acidic supports, such as ASA or Al-SBA-15, the performance of the Mo oxide catalysts is close to that of Pt supported catalysts, with high isomer yield (~60% for both Pt and Mo based catalysts). This demonstrates that Mo oxide catalysts supported on mildly acidic mesoporous supports such as ASA behave and perform similarly to the noble-metal Pt catalyst under the same conditions.

3.2.4. Influence of the ratio n metal surface /n acid

The optimal loading of metal allowing to fulfill the (de)hydrogenation step was demonstrated with respect to the amount of acid sites in the case of Pt-solid acid bi-functional catalyst. The influence of this ratio and its optimum value have been extensively studied for Pt [3,39]. In the case of MoO_x-based catalysts (Table 1, row 3,7,8), the *n Metal surface /n Acid* ratio was determined in order to study its influence of the catalysis performance (Fig.SI.6) The

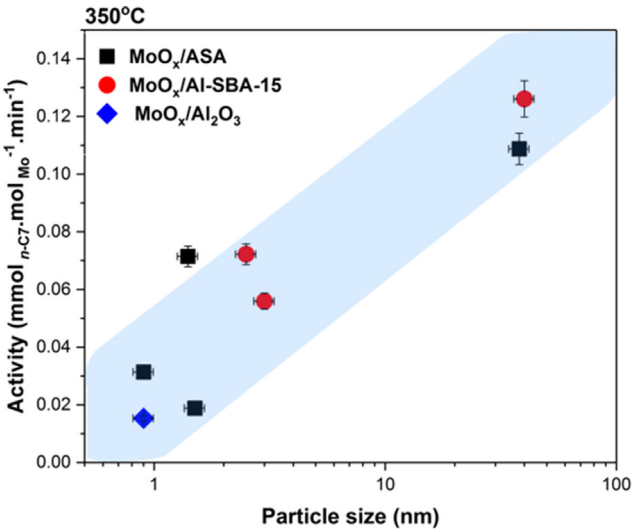

Fig. 6. Influence of the particles size on activity for Mo supported catalysts on various supports (at 350 °C) Particles size axis is plotted in logarithmic scale. Particle sizes are from XRD crystallites size for larger particles (30–40 nm) and from TEM for smaller (<20 nm) NPs. Samples 3,6,8,11,15–17 referred in Table 1 (blue shading is a guide for the eye).

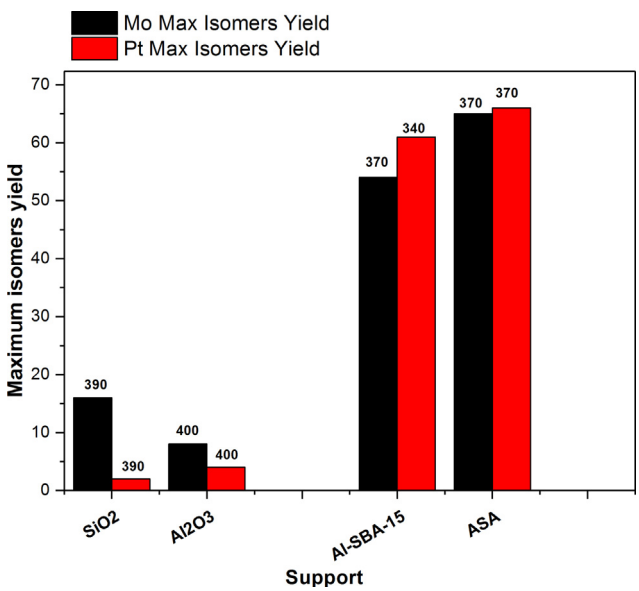

Fig. 7. Overview of the maximum isomers yield of both Mo and Pt supported catalysts on various porous supports (temperature on top of each column). All Mo catalysts were prepared by physical mixture with MoO_3 powder. All Pt sample were prepared by IE method with the exception of Pt/Al_2O_3 that was obtained from a commercial supplier.

activity of MoO_x/ASA increased slightly with a higher metal to acid ratio. A ratio of *n MoO₂ surface/ n acid* around 0.13 is enough to obtain a well-balanced Mo catalyst, this value is higher than the optimal ratio *n Pt surface/ n acid* that is around 0.03. This suggests that the activity of Mo for (de)hydrogenation is lower than for Pt, with a higher amount of metal oxide sites required (See Fig SI.6).

3.2.5. Bi-functional mechanism

Due to the acidity of the Mo oxide, it is possible to perform the hydroisomerization without additional solid acid, as reported earlier by Ledoux and co-workers [16]. Indeed, MoO_x powder reduced under H_2 shows activity but with a limited isomer formation under our reaction conditions (Fig. 8). Interestingly, the addition of a porous solid acid catalyzing the isomerization/cracking steps of the reaction gives a significant improvement in the performance of the catalyst and exhibits a bi-functional mechanism similar to that seen in typical hydrocracking catalysts with a typical product distribution. The bifunctional properties of the MoO_x catalysts were probed by mixing a sieved fraction (75–212 μm) of MoO_x powder with a similar sieved fraction of ASA solid acid. As can be seen in Fig. 8, adding the solid acid ASA to the molybdenum oxide powder led to an increase in the isomer yield from 31% to 50%. This suggests a synergy between the MoO_3, acting as (de)hydrogenation function and providing alkenes, and the acid sites, responsible for isomerization or cracking. The grain mixed catalyst showed a higher maximum isomer yield than the MoO_3 powder alone, yet not as high as for the MoOx/ASA (PM) catalyst discussed previously. This preparation technique by physical mixture results in a more intimate proximity between the MoO_x crystals and the solid acid, when compared to the catalyst prepared by grains mixing. The MoOx/ASA (PM) catalyst should therefore result in an average distance between the two functions of hundreds of nm, that should fulfill the Weisz intimacy criterion [40] (influence of the distance between metal and acid sites for an optimal activity in the case of bi-functional catalysts).

As the Mo catalysts present interesting properties, and increased performance when the metal-to-acid distance is decreased below micrometers, we prepared a MoO_x/ASA catalyst by extrusion of the two powders using only distilled water as formulation medium. The extrudate catalyst showed performance similar to the physical mixture catalyst; indicating the possibility of a facile scale-up of the catalyst preparation for industrial application (See Fig. 8).

3.2.6. Nature of the MoO_x active sites

Previous reports suggest the gradual formation of an active carbide phase of Mo under a pentane/H_2 flow [17]. A catalyst was therefore prepared by physical mixture of Mo_2C to compare with our MoO_x/ASA samples, but this catalyst resulted in very low conversions, and no isomer formation in *n*-heptane conversion (Fig SI.8). As our standard catalysis procedure involved step by step increasing of the temperature with time on stream, we investigated the possibility of a carbide phase formation under the heptane feed by investigating MoO_x/ASA directly at higher temperature (Fig SI.9). Still, the same low level of conversion and isomers yield were obtained. This ruled out the impact of an activation period under *n*-C7/H_2 flow. The stability of the catalyst and the absence of deactivation over 150 h hour catalysis was also checked by measuring the conversion at lower temperature at the end of the run. XRD characterization of the used catalysts did not reveal diffraction peaks of Mo carbides but only of Mo oxides (See Fig. 3). Therefore, we can rule out the formation of an active phase based on crystalline Mo carbide or Mo oxycarbide during the catalysis; the active phase for the (de)hydrogenation is likely Mo oxide. We also performed Raman spectroscopy on these catalysts, since this technique allows to study amorphous Mo oxide, and to investigate the coordination of Mo-O compared to the commercial MoO_3 powder (Fig SI.10.) [41–43]. In our case, the large number of different vibration and stretching signals did not allow us to conclude on one single coordination mode of the oxide, but it confirmed the presence of $MoO_2(=O_2)_2$, that is Mo oxide species coordinated to oxygen and other MoO_x species.

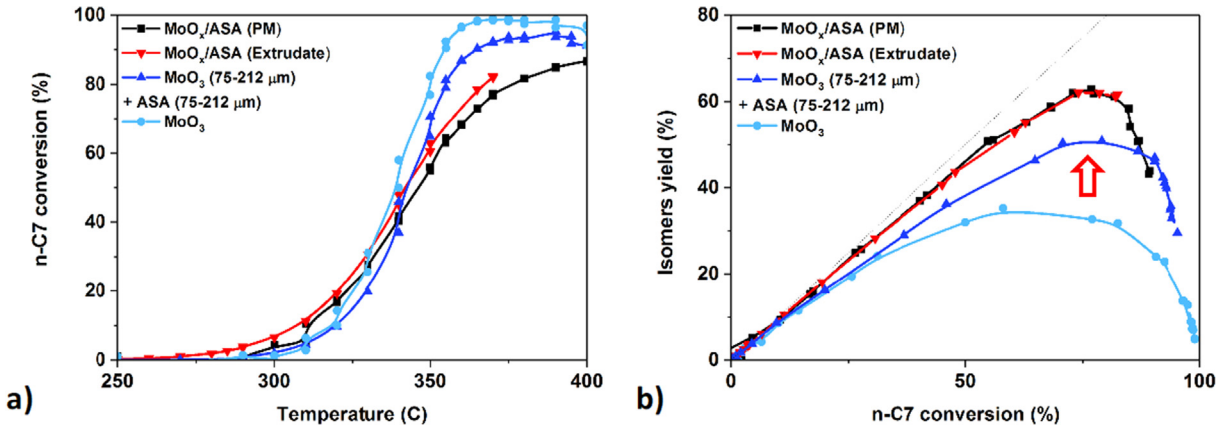

Fig. 8. a) n-heptane conversion as a function of the temperature for MoO_3/ASA catalyst (prepared by physical mixture (PM) or by extrusion (Extrudate); unsupported MoO_3 powder and grain mixing of ASA and MoO_3 powder (75–212 μm) b) Isomers yield as a function of n-heptane conversion (10 bar ; H_2/n-C7 = 10/1 mol/mol; WHSV = 1.15 $g_{n\text{-}C7}.g_{catalsyt}.h^{-1}$) The arrow indicates the increase in isomers yield upon addition of a solid acid to the MoO_x catalyst.

4. Conclusion

Supported molybdenum oxide catalysts were prepared and studied for *n*-heptane hydroconversion as a model feedstock for alkane conversion. The optimized catalyst was a physical mixture of the MoO_3 oxide and an acidic mesoporous silica-alumina. This catalyst exhibited Pt-like performance, although with a higher weight loading of Mo, under industrially relevant conditions, showing that a non-noble metal oxide-based catalyst can be a used as an efficient substitute for hydroisomerization of alkanes. A bi-functional mechanism with Mo oxide as (de)hydrogenation function and silica-alumina as acid function was demonstrated, with the active phase for (de)hydrogenation assumed to be crystallites of MoO_2. We could demonstrate the industrial relevance of MoO_x catalysts as the extrudate sample showed similar performance; indicating the possibility of a facile scale-up of the catalyst preparation. These results are of great interest in the field of research on non-sulfided catalysts for upgrading of high-molecular weight hydrocarbons. Therefore, future research will involve studies with heavier feedstocks (such as FT wax) on these Mo-oxide bifunctional catalysts.

Declaration of Competing Interest

The authors declare that they have no known competing financial interests or personal relationships that could have appeared to influence the work reported in this paper.

Acknowledgments

Miguel Rivera-Torrente is acknowledged for assistance with the Raman measurements and for BET measurements. Lars van der Wal for TEM measurements. BP plc is acknowledged for funding.

Appendix A. Supplementary material

Supplementary data to this article can be found online at https://doi.org/10.1016/j.jcat.2020.08.004.

References

[1] J. Weitkamp, Catalytic hydrocracking-mechanisms and versatility of the process, ChemCatChem 4 (3) (2012) 292–306, https://doi.org/10.1002/cctc.201100315.
[2] L.B. Galperin, S.A. Bradley, T.M. Mezza, Hydroisomerization of n -decane in the presence of sulfur effect of metal, Acid Bal. Metal Locat. 219 (2001) 79–88.
[3] M. Guisnet, F. Alvarez, G. Giannetto, G. Perot, Hydroisomerization and hydrocracking of N-heptane on Pth zeolites. Effect of the porosity and of the distribution of metallic and acid sites, Catal. Today 1 (4) (1987) 415–433, https://doi.org/10.1016/0920-5861(87)80007-X.
[4] J.M. Grau, J.M. Parera, Conversion of heavy N-alkanes into light isomers over H-mordenite, platinum/H-mordenite, platinum/alumina and composite catalysts, Appl. Catal. A, Gen. 106 (1) (1993) 27–49, https://doi.org/10.1016/0926-860X(93)80154-I.
[5] A. Jentys, Characterization of metallic species on Ni- And Co-containing ZSM-5 catalysts - reduction behavior and catalytic properties, Zeolites 18 (5–6) (1997) 391–397, https://doi.org/10.1016/S0144-2449(97)00030-4.
[6] A. Lugstein, A. Jentys, H. Vinek, Hydroisomerization and cracking of N-octane and C8 isomers on Ni-containing zeolites, Appl. Catal. A Gen. 176 (1) (1999) 119–128, https://doi.org/10.1016/S0926-860X(98)00231-2.
[7] M.S. Rana, V. Sámano, J. Ancheyta, J.A.I. Diaz, A review of recent advances on process technologies for upgrading of heavy oils and residua. Fuel 2007, 86 (9 SPEC. ISS.), 1216–1231. https://doi.org/10.1016/j.fuel.2006.08.004.
[8] A.A. Pimerzin, A.A. Roganov, S.P. Verevkin, M.E. Konnova, V.A. Pilshchikov, A.A. Pimerzin, Bifunctional catalysts with noble metals on composite Al2O3-SAPO-11 carrier and their comparison with CoMoS One in n-hexadecane hydroisomerization, Catal. Today 2019 (329) (2018) 71–81, https://doi.org/10.1016/j.cattod.2018.12.034.
[9] Klerk, A. de. Catalysis in the Refining of Fischer–Tropsch Syncrude Upgrading of Fischer – Tropsch Oxygenates; 2010.
[10] International Chamber of Shipping. Compliance with the 2020 ' Global Sulphur Cap .' Int. Chamb. Shipp. 2019, No. July 2019, 40.
[11] R.B. Levy, M. Boudart, Platinum-like behavior of tungsten carbide in surface catalysis, Science (80-.). 1973, 181, 547–549.
[12] F.H. Ribeiro, M. Boudart, R.A. Dalla Betta, E. Iglesia, Catalytic reactions of N-alkanes on β-W2C and WC: the effect of surface oxygen on reaction pathways, J. Catal. 130 (2) (1991) 498–513, https://doi.org/10.1016/0021-9517(91)90131-M.
[13] J.S. Lee, L. Volpe, F.H. Ribeiro, M. Boudart, Molybdenum carbide catalysts. II. Topotactic synthesis of unsupported powders, J. Catal. 112 (1) (1988) 44–53, https://doi.org/10.1016/0021-9517(88)90119-4.
[14] M.J. Ledoux, C. Pham-Huu, H. Dunlop, J. Guille, N-Hexane isomerisation on high surface specific Mo2C activaitesd by an oxidative treatment, New Front. Catal. (1993) 19–24.
[15] E.A. Blekkanj, C. Pham-huu, M.J. Ledoux, J. Guillet, Isomerization of N-heptane, Ind. Eng. Chem. Res. 33 (1994) 1657–1664, https://doi.org/10.1021/ie00031a003.
[16] A.P.E. York, C. Pham-Huu, P. Del Gallo, M.J. Ledoux, Molybdenum oxycarbide hydrocarbon isomerization catalysts: cleaner fuels for the future, Catal. Today 35 (1–2) (1997) 51–57, https://doi.org/10.1016/S0920-5861(96)00134-4.
[17] M.J. Ledoux, C.P. Huu, J. Guille, H. Dunlop, Compared activities of platinum and high specific surface area Mo2C and WC catalysts for reforming reactions. I. Catalyst activation and stabilization: reaction of n-hexane, J. Catal. 134 (2) (1992) 383–398, https://doi.org/10.1016/0021-9517(92)90329-G.
[18] P. Delporte, F. Meunier, C. Pham-Huu, P. Vennegues, M.J. Ledoux, J. Guille, Physical characterization of molybdenum oxycarbide catalyst; TEM XRD and XPS, Catal. Today 23 (3) (1995) 251–267, https://doi.org/10.1016/0920-5861(94)00166-Y.
[19] Marc-Jacques Ledoux; Jean-Louis Guille; Cuong Pham-Huu; Sophie Marin. Production of Heavy Metal Carbides of High Specific Surface Area. USOO5308597A, 1994.
[20] M.-J. Ledoux, J.-L. Guille, C.P. Huu, H. Dunlop, M. Prin, Preparation of a catalyst from metal oxide by reduction and partial carburization by reaction gases, USOO5468370A (1995).
[21] C. Bouchy, C. Pham-Huu, B. Heinrich, C. Chaumont, M.J. Ledoux, Microstructure and characterization of a highly selective catalyst for the isomerization of alkanes: a molybdenum oxycarbide, J. Catal. 190 (1) (2000) 92–103, https://doi.org/10.1006/jcat.1999.2741.

[22] C. Pham-Huu, P. Gallo Del, E. Peschiera, M.J. Ledoux, N-hexane and n-heptane isomerization at atmospheric and medium pressure on MoO3-carbon-modified supported on SiC and γ-Al2O3, Appl. Catal. A, Gen. 132 (1) (1995) 77–96, https://doi.org/10.1016/0926-860X(95)00151-4.
[23] M.J. Ledoux, P. Del Gallo, C. Pham-Huu, A.P.E. York, Molybdenum oxycarbide isomerization catalysts for cleaner fuel production, Catal. Today 27 (1996) 145–150, https://doi.org/10.1016/0920-5861(95)00182-4.
[24] C. Bouchy, C. Pham-Huu, B. Heinrich, E.G. Derouane, S.B. Derouane-Abd Hamid, M.J. Ledoux, In situ TPO, TPD and XRD characterisation of a molybdenum oxycarbohydride catalyst for n-butane isomerisation, Appl. Catal. A Gen. 215 (1–2) (2001) 175–184, https://doi.org/10.1016/S0926-860X(01)00532-4.
[25] L.O. Alemán-Vázquez, E. Torres-García, J.R. Villagómez-Ibarra, J.L. Cano-Domínguez, Effect of the particle size on the activity of MoO x C y catalysts for the isomerization of heptane, Catal. Letters 100 (3–4) (2005) 219–226, https://doi.org/10.1007/s10562-004-3459-0.
[26] L.O. Alemán-Vázquez, F. Hernández-Pérez, J.L. Cano-Domínguez, A. Rodríguez-Hernández, J.L. García-Gutiérrez, Binder effect on the catalytic activity of MoO3 bulk catalyst reduced by H2 for N-heptane hydroisomerization, Fuel 117 (PART A) (2014) 463–469, https://doi.org/10.1016/j.fuel.2013.08.085.
[27] P. Wehrer, C. Bigey, L. Hilaire, Catalytic reactions of N-hexane and 1-hexene on molybdenum dioxide, Appl. Catal. A Gen. 243 (1) (2003) 109–119, https://doi.org/10.1016/S0926-860X(02)00543-4.
[28] P. Wehrer, L. Hilaire, E. Petit, Influence of the reduction conditions of MoO3on its isomerizing properties, Appl. Catal. A Gen. 273 (1–2) (2004) 249–258, https://doi.org/10.1016/j.apcata.2004.06.050.
[29] P. Wehrer, S. Libs, L. Hilaire, Isomerization of Alkanes and alkenes on molybdenum oxides, Appl. Catal. A Gen. 238 (1) (2002) 69–84, https://doi.org/10.1016/S0926-860X(02)00216-8.
[30] A. Goguet, S. Shekhtman, F. Cavallaro, C. Hardacre, F.C. Meunier, Effect of the carburization of MoO3-based catalysts on the activity for butane hydroisomerization, Appl. Catal. A Gen. 344 (1–2) (2008) 30–35, https://doi.org/10.1016/j.apcata.2008.03.038.
[31] J. Harmel, Wal L.I. Van Der, P.E. De Jongh, K.P. De Jong, Influence of intimacy for metal-mesoporous solid acids catalysts for n-alkanes hydro-conversion, Catal. Sci. Technol. (2020), https://doi.org/10.1039/c9cy02510c.
[32] K. Cheng, L.I. van der Wal, H. Yoshida, J. Oenema, Z. Zhang, G. Sunley, J. Zečević, K.P. de Jong, J. Harmel, Impact of the spatial organization of bifunctional metal-zeolite catalysts for hydroisomerization of light alkanes, Angew. Chemie Int. Ed. (2019), https://doi.org/10.1002/anie.201915080.
[33] J.A.R. Van Veen, A method for the quantitative determination of the basic hydroxyl groups on an alumina surface, J. Colloid Interface Sci. 121 (1) (1988) 214–219, https://doi.org/10.1016/0021-9797(88)90425-0.
[34] M. Guisnet, "ideal" bifunctional catalysis over Pt-acid zeolites, Catal. Today 218–219 (2013) 123–134, https://doi.org/10.1016/j.cattod.2013.04.028.
[35] N. Batalha, L. Pinard, C. Bouchy, E. Guillon, M. Guisnet, N-Hexadecane hydroisomerization over Pt-HBEA catalysts. quantification and effect of the intimacy between metal and protonic sites, J. Catal. 307 (2013) 122–131, https://doi.org/10.1016/j.jcat.2013.07.014.
[36] H.J. Robota, J. Jones, M. Luo, A. Stewart, Hexadecane hydrotreating as a surrogate for Fischer-Tropsch wax upgrading to aviation fuel using a Co/MoO_3/silica-alumina catalyst, ACS Symp. Ser. 1084 (2011) 279–287, https://doi.org/10.1021/bk-2011-1084.ch012.
[37] W. Böhringer, A. Kotsiopoulos, M. de Boer, C. Knottenbelt, J.C.Q. Fletcher, Selective Fischer-Tropsch wax hydrocracking – opportunity for improvement of overall gas-to-liquids processing, Stud. Surf. Sci. Catal. 163 (2007) 345–365.
[38] X. Carrier, J.F. Lambert, M. Che, Ligand-promoted alumina dissolution in the preparation of MoO(x)/γ-Al_2O_3 catalysts: evidence for the formation and deposition of an anderson-type alumino heteropolymolybdate, J. Am. Chem. Soc. 119 (42) (1997) 10137–10146, https://doi.org/10.1021/ja971981r.
[39] F. Alvarez, F.R. Ribeiro, G. Perot, C. Thomazeau, M. Guisnet, Hydroisomerization and hydrocracking of alkanes, J. Catal. 162 (2) (1996) 179–189, https://doi.org/10.1006/jcat.1996.0275.
[40] P.B. Weisz, E.W. Swegler, Stepwise reaction on separate catalytic centers: isomerization of saturated hydrocarbons, Science (80-.) 126 (1957) 31–32.
[41] J. Gao, Y. Zheng, J.-M. Jehng, Y. Tang, I.E. Wachs, S.G. Podkolzin, Identification of molybdenum oxide nanostructures on zeolites for natural gas conversion, Science (80-.) 348 (6235) (2015) 686–690, https://doi.org/10.1126/science.aaa7048.
[42] A. Chakrabarti, I.E. Wachs, Molecular structure-reactivity relationships for olefin metathesis by Al_2O_3 – supported surface Mo_O x sites, ACS Catal. acscatal.7b03598 (2017), https://doi.org/10.1021/acscatal.7b03598.
[43] K. Amakawa, L. Sun, C. Guo, M. Hävecker, P. Kube, I.E. Wachs, S. Lwin, A.I. Frenkel, A. Patlolla, K. Hermann, et al., How strain affects the reactivity of surface metal oxide catalysts, Angew. Chemie - Int. Ed. 52 (51) (2013) 13553–13557, https://doi.org/10.1002/anie.201306620.